

Christopher M. Godfrey\*

University of North Carolina at Asheville, Asheville, North Carolina

Christopher D. Karstens

NOAA/NWS/SPC, Norman, Oklahoma

Daniel Rhee

University of Illinois at Urbana–Champaign, Urbana, Illinois

Chris J. Peterson

University of Georgia, Athens, Georgia

Franklin T. Lombardo

University of Illinois at Urbana–Champaign, Urbana, Illinois

## 1. INTRODUCTION

As part of the ongoing effort to produce a standard for wind speed estimation (LaDue et al. 2018), the authors have developed three techniques to estimate wind speeds from tornadoes based on either discernible patterns of treefall or the severity of damage within forested areas: the Lombardo, Karstens, and Godfrey–Peterson methods. While each method produces reasonable wind speed estimates for individual tornado tracks, as shown by their respective published results, the authors wondered whether the methods would produce comparable results for the same tornado. The 22 May 2011 Joplin, MO EF5 tornado analyzed by Karstens et al. (2013) and Lombardo et al. (2015) provides a unique opportunity to develop a comparison of the EF-scale estimates provided by each of these three methods. Since the Lombardo and Karstens methods had already been applied to this tornado track, only the Godfrey–Peterson approach to wind speed estimation remained in order to compare all three methods. Additionally, a detailed ground assessment of mostly traditional EF-scale damage indicators exists along the entire damage track (Marshall et al. 2012), enabling a complete comparison between all three methods along with an objective estimate for ground truth.

These three treefall pattern and forest damage analysis methods for wind speed estimation rely on observed tornado damage to a collection of trees, which must have been uprooted or snapped. While all three methods estimate the tornado wind speed by analyzing the tree damage as a collective, the Lombardo and Karstens methods require that the treefall vectors reveal a pattern. Application of both the Lombardo and Karstens methods requires the creation of a detailed database of digitized, georeferenced treefall vectors, collected through

field surveys or high-resolution aerial imagery. The best match between the treefall patterns identified through a mapping of these vectors and treefall patterns produced by a simulated wind field of comparable geospatial scale provides an estimate of the wind speed from the tornado. In contrast, the Godfrey–Peterson method does not require a simulated wind field or treefall vectors, but instead uses the results of a coupled wind and tree resistance model to estimate the most probable wind speed associated with distinct levels of forest damage. Each of these three methods can provide wind speed estimates for all or part of a tornado track.

## 2. WIND SPEED ESTIMATION METHODS

The Godfrey–Peterson method is based on the work of Godfrey and Peterson (2017); the Lombardo method is based on the work of Kuligowski et al. (2014), Lombardo et al. (2015), and Rhee and Lombardo (2018); and the Karstens method is based on the work of Karstens et al. (2013). The essential first component for both the Lombardo and Karstens methods is an idealized axisymmetric vortex model to simulate a single vortex tornado. Note that the Godfrey–Peterson method does not require a vortex model and is the only method that can be applied to a multiple-vortex tornado. Implementation of the vortex model has generally been implemented using the Rankine assumption, following equations provided in Holland et al. (2006; note the error in Eq. 11 of this article) and Beck and Dotzek (2010), though the earliest work in this domain is that of Letzmann (1923, 1925, 1939). Both Karstens et al. (2013) and Lombardo et al. (2015) outline additional assumptions and simplifications to the Rankine vortex for the respective wind speed estimation methods. In both cases, the Rankine vortex neglects the vertical wind component and the vertical distribution of horizontal winds (i.e., the vertical wind profile) and thus represents a horizontal, two-dimensional wind field that does not vary with height

---

\*Corresponding author address: Christopher M. Godfrey, University of North Carolina at Asheville, Department of Atmospheric Sciences, One University Heights, CPO #2450, Asheville, NC 28804; e-mail: cgodfrey@unca.edu.

above the ground within the 30-50 m height of the trees. The Lombardo and Karstens methods vary the following parameters in vortex simulations to achieve a “best match” (i.e., subjective best-fit) to observed tree damage patterns: tangential velocity, translational velocity, radial velocity (typically inflow), radius of maximum rotational velocity, and direction of movement of the vortex.

Each method compares observed and simulated treefall using a variety of approaches. For each tree, the wind velocity is either input into a tree stability model (Godfrey–Peterson method) or compared with an average treefall-inducing wind speed (Lombardo method) or an assigned wind speed from a Gumbel distribution (Gumbel 1958) of critical treefall-inducing wind speeds (Karstens method). If that velocity results in force values greater than either the assumed root resistance or trunk resistance, the tree fails and falls in the direction of the instantaneous wind vector. These methods assume no cumulative weakening of trees from exposure to sustained winds. Each tree is independent of neighboring trees, neither benefiting from shelter or interlocking branches, nor suffering greater risk from the impact of falling neighbors. While useful in any setting, the Lombardo and Karstens methods may therefore be most applicable to small patches or groves of trees (near the size of one hectare), while the Godfrey–Peterson method may be more applicable to large, continuous expanses of forests.

The potential role of topography is an important consideration in the application of these wind speed estimation methods. While none of the implementations to date have explicitly considered topography or terrain, there is evidence from several directions that suggests such effects are very important. First, full-physics simulations that include even single hills or ridges greatly increase

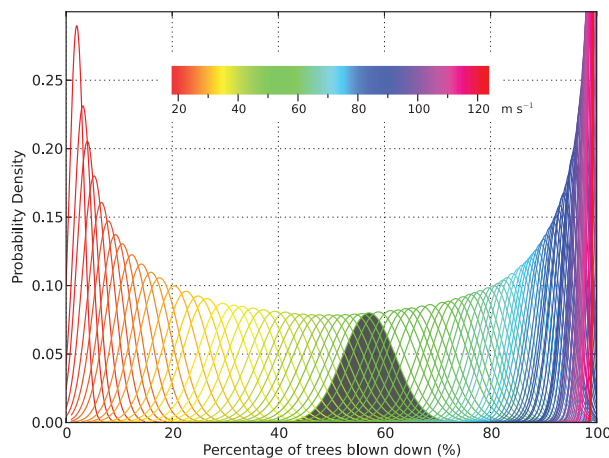


FIG. 1. Probability density functions describing the percentage of trees blown down at various wind speeds in 10000 fictitious sample plots using trees drawn from a database of observed trees in the Great Smoky Mountains National Park. The shaded region corresponds with a most probable wind speed of  $50 \text{ m s}^{-1}$  in this forest. From Godfrey and Peterson (2017).

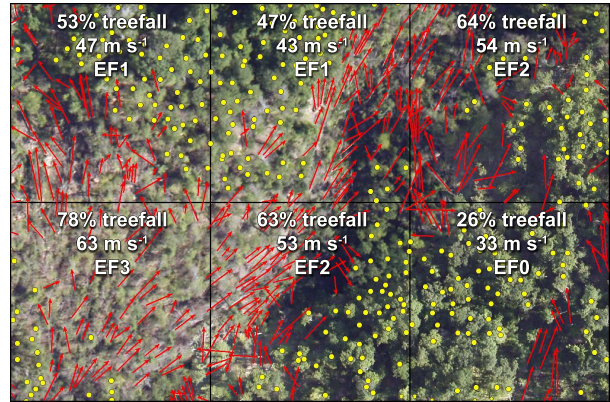


FIG. 2. A section of a tornado track illustrating the assignment procedure for EF-scale levels. Red arrows represent fallen trees, yellow dots represent standing trees, and the black lines show the boundaries of the  $100 \text{ m} \times 100 \text{ m}$  subplots. At the top left, for example, the tornado knocked down 53% of the trees in the subplot, corresponding with a most probable wind speed of  $47 \text{ m s}^{-1}$  ( $105 \text{ m.p.h.}$ ) and an EF-scale rating of EF1. From Godfrey and Peterson (2017).

the complexity of the near-ground wind field (Lewellen 2012) to the point where general patterns become difficult to identify. Second, observations by the authors of actual treefall directions of hundreds of thousands of trees in a 2011 Great Smoky Mountains tornado are exceedingly complex, and appear to defy simple description. Indeed, Godfrey and Peterson (2017) note that the Holland et al. (2006) approach should not be attempted in rugged terrain, and is most promising in low-relief landscapes. Regarding the methods presented here, the Lombardo method follows a similar sensitivity to individual treefall, and thus, sensitivity to rugged terrain, whereas the Godfrey–Peterson and Karstens methods will have less sensitivity to the underlying terrain due to the reliance on aggregated treefall. In fact, the Godfrey–Peterson method is particularly useful in regions with complex topography.

## 2.1 Godfrey–Peterson Method

The Godfrey–Peterson method follows the approach of Godfrey and Peterson (2017) and applies to damage tracks through generally continuous sections of forested land, regardless of topographical features. At its core, this statistical approach relies on a coupled wind and tree resistance model (Peltola and Kellomaki 1993) to develop a distribution of treefall percentages associated with a given wind speed in a particular forest. Tree stability models calculate the force of the wind on a tree based on knowledge of its species, height, trunk diameter at 1.4 m above the ground [i.e., diameter at breast height (DBH)], and either observed or inferred crown width and depth. The force of the wind is further dependent on the wind velocity, air density, and drag coefficient and results in a mechanical displacement of the crown, causing a bending moment at the base of the tree. If this bend-

ing moment exceeds the tree's resistance to breakage or uprooting, then the tree falls. An individual tree's DBH and known species-dependent values for wood strength (Kretschmann 2010; Panshin and de Zeeuw 1970) provide estimates for the critical bending moment for trunk breakage, while empirical winching studies (Kane and Smiley 2006; Nicoll et al. 2006; Peltola 2006; Peterson and Claassen 2013) allow estimates of the critical bending moment for uprooting. The area of the crown depends on a species-dependent height–DBH allometry based on the ideal tree distribution (ITD) model (Purves et al. 2007). Godfrey and Peterson (2017) explain the implementation of the ITD model in this context.

With knowledge of the forest composition, tree size distribution, and tree density determined through ground surveys either before or after a tornado event, the method proceeds by randomly drawing, with replacement, a small sample of 100 trees from this database of observed trees. The coupled wind and tree resistance model determines the percentage of trees that fall in this fictitious plot for a set of wind speeds ranging from light breezes to extreme wind speeds. Repeating this process a sufficient number of times (i.e., 10000 times) yields a probability density function that describes treefall percentages for each wind speed (Fig. 1). In small sections of a tornado track (e.g., square plots measuring 100–200 m on each side), the assignment of wind speeds proceeds by assessing the observed percentage of fallen trees. The most probable wind speed that produced the damage in each subplot then corresponds with the associated sampling distribution with its peak matching the observed percentage of trees blown down in that forest section. Fig. 2 illustrates this procedure.

It is important to note that implementation of this method does not strictly require ground surveys to ascertain the species composition, tree size distribution, and tree density along or near the tornado track, nor does it require the use of the tree stability model and resampling procedure described above. These elements and tools are required for the development of a new set of probability density functions that relate the percentage of trees blown down with wind speed in a new forest. If time, resources, or expertise limit the ability to conduct ground surveys and develop new functions, then it remains reasonable to use existing functions developed for different forests under the assumption that the species composition and size distribution is reasonably similar. In lieu of extensive ground surveys, models, and statistical procedures, the wind speed–treefall percentage relationship based on the species composition, tree size distribution, and tree density observed through ground surveys in the Great Smoky Mountains National Park (Godfrey and Peterson 2017) could be used immediately in a different location. Tree winching studies that measure the torque required to knock down trees suggest that the wind speed required for treefall is not substantially different across species and size classes (Cannon et al. 2015). Indeed, in the two forests studied by Godfrey and Peterson (2017),

only very slight differences are evident in the probability density functions for the Great Smoky Mountains National Park and the Chattahoochee National Forest. The wind speed–treefall percentage relationship found by Godfrey and Peterson (2017), therefore, may have broad applicability to other forests, but detailed ground survey information to date is unknown. If the wind speed–treefall percentage relationship is known or can be approximated for the forest under consideration, then a damage assessment team simply needs to estimate the percentage of fallen trees within a plot of the appropriate area, provided the plot contains a sufficient number of trees (i.e., more than at least 10). Ideally, more than 100 total trees will be present within the sample plot of the appropriate area. Lastly, Godfrey and Peterson (2017) note that this wind speed estimation technique allows for the calculation of confidence intervals on each wind speed estimate. This allows a damage assessment team to adjust EF-scale levels upward or downward depending on other factors such as soil or rooting conditions, the age or exposure of the tree stand, or other specific circumstances surrounding a tornado event.

## 2.2 Lombardo Method

The Lombardo method determines the near-surface wind speeds of the tornado by analyzing the treefall pattern that the tornado produces. The method uses a Rankine vortex model to replicate the tornado wind field and the treefall pattern to estimate the parameters of the wind field. Rhee and Lombardo (2018) discuss further improvements through the use of an asymmetric vortex

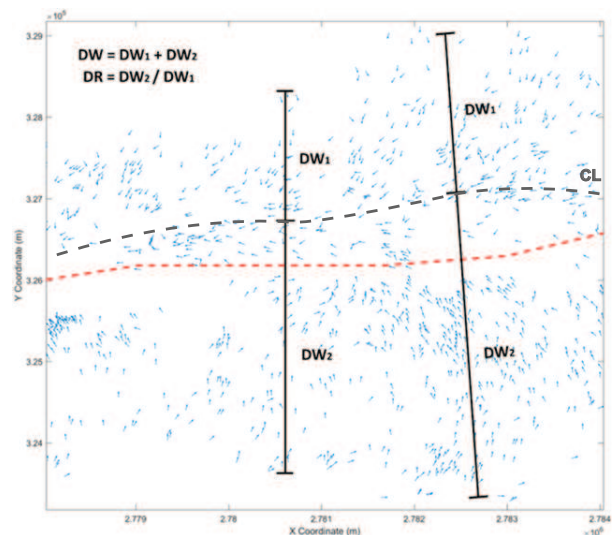


FIG. 3. Treefall pattern diagnostics and digitized treefall vectors for the 22 May 2011 Joplin, MO tornado, including the damage width (DW) on either side of the confluence line (CL, gray dashed). The red dashed line indicates the half-way point across the damage path. DW1 and DW2 refer to the damage width above the CL and below the CL, respectively.

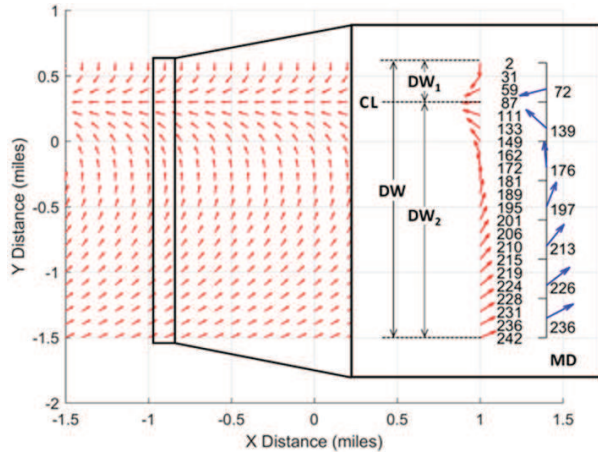


FIG. 4. Treefall pattern diagnostics for a simulated treefall pattern. Blue arrows indicate the meteorological wind direction (MD) at defined points along the transect. Other symbols are as defined in Fig. 3. From Rhee and Lombardo (2018).

model and radar measurements and the application of this method in crop and structural infrastructure damage. To implement the method, a user first obtains the observed treefall pattern of a tornado through either aerial photographs or a ground survey and then generates a simulated treefall pattern that resembles the observed pattern through iteration with different vortex parameters. Quantification of the treefall pattern into a set of diagnostics, along with the calculation of the mean-squared error between the observed and simulated patterns, allows the selection of the most appropriate parameters for the Rankine model. The set of diagnostics for the treefall pattern include 1) the width of the tree damage (damage width, DW), 2) the ratio of the damage width (damage ratio, DR) on either side of the confluence line (CL, i.e., the location where the treefall patterns converge) in a given transect, and 3) the azimuth (or average azimuth) of treefall at a specific location within the transect (meteorological direction, MD). Fig. 3 illustrates the observed treefall pattern diagnostics for a portion of the Joplin tornado track, while Fig. 4 shows the same diagnostics for the simulated treefall pattern.

A comparison between the diagnostics from the observed and simulated treefall patterns allows the determination of the best Rankine model parameters. In the Lombardo method, the average treefall-inducing wind speed is one of the input variables required to produce a simulated treefall pattern. The scientific literature (Peltola and Kellomaki 1993; Peltola et al. 1999) provides an estimate of the initial wind speed input range, which is refined iteratively until the modeled treefall pattern best matches the observations. This approach assumes that trees fall in the direction of the wind when the wind speed exceeds the critical treefall-inducing wind speed. The parameter determination process iterates until the discovery of the minimum mean-squared error between the two diagnostics. Fig. 5 demonstrates the comparison

between the damage width and damage ratio for the observed and simulated patterns for the Joplin tornado. The “best-matching” combination of Rankine model parameters that produces the minimum total error for both diagnostics allows a reconstruction of the wind field, from which a user can determine the maximum wind speed of the tornado. For example, Fig. 6 shows the time history of wind speed and direction of the reconstructed wind field for the Joplin tornado at the southeast corner of the intersection of W. 26th St. and S. Jackson Ave.

While the Lombardo method does not require them, ground surveys are recommended if possible as a supplement to, or in lieu of, aerial photographs since detailed data collection on the ground can provide information that is often unobtainable from the air, such as DBH, height, species, and other tree characteristics. Generally, a surveyor will document the location and azimuth of fallen trees within multiple transects perpendicular to the tornado track. In addition to treefall, a detailed survey of failed and non-failed traffic signs may also provide the lower and upper bound wind speeds of the tornado, respectively.

### 2.3 Karstens Method

The Karstens method represents an objective procedure to estimate a peak wind speed from a tornado after performing a detailed analysis of observed treefall from a section of a tornado damage path where the most intense treefall occurred. This method matches observed- and model-average cross-sectional treefall vectors and extends the work of Holland et al. (2006) and Beck and Dotzek (2010), while adding additional geospatial, statistical, and pattern-recognition techniques to estimate the peak wind speed associated with tornado-induced treefall patterns.

The Karstens method requires georeferenced vertical aerial imagery with sufficient resolution to identify fallen trees, as well as an area along a tornado track that has a sufficient homogeneous coverage of trees such that a damaged region is evident in the aerial photographs. The process for applying this method to a region of tornado-induced treefall first involves the creation of four geospatial vector datasets. These include digitized treefall vectors, a damage path polygon, a line of maximum damage, and an estimation of the observed tornado centroid loca-

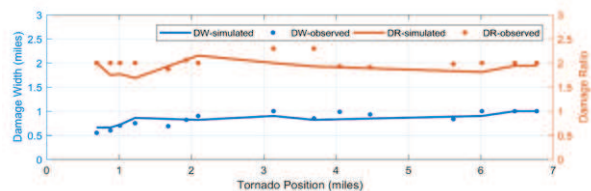


FIG. 5. Damage width (blue) and damage ratio (orange) comparisons between the observed (dots) and simulated (solid line) treefall patterns for the 22 May 2011 Joplin, MO tornado.

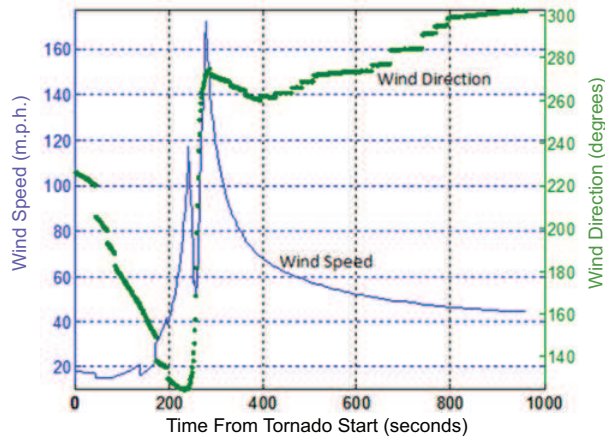


FIG. 6. Wind speed and direction time history for the 22 May 2011 Joplin, MO tornado wind field at the southeast corner of the intersection of W. 26th St. and S. Jackson Ave.), using the “best-matching” parameters. From Kuligowski et al. (2014).

tions (i.e., the center of mesocyclone circulation obtained from radar data) at various positions along the entirety of the damage path. Fig. 7 illustrates each of these four required datasets. The line of maximum damage should be estimated from aerial imagery and corroborated with a ground survey, if possible. As discussed in Karstens et al. (2013), this line may be interchanged with, but is not necessarily equivalent to, the approximate tornado centerline. A user first segments this line of maximum damage along the track based on its intersection with the nearest estimated tornado centroid locations. Thereafter, the user segments the line of maximum damage into 1 s increments based on the amount of time between estimated tornado locations, such that the direction of translation can be estimated at fine spatial and temporal resolution between each segment. Then, the user pairs each digitized tree residing within the digitized damage path poly-

gon with the nearest translation segment, allowing for the calculation of the distance from maximum damage and the calculation of a normalized treefall direction. This normalization procedure is necessary to produce an observational dataset that more closely resembles the patterns of treefall produced by the Rankine vortex model that uses a unidirectional translation vector. This procedure therefore removes from consideration fallen trees residing outside of the digitized damage path polygon. Frequently, these exterior regions will contain a low sample size of trees, thus making any results sensitive to outliers. Notably, Karstens et al. (2013) found evidence of a rear-flank downdraft surge that may have led to a more divergent pattern of treefall on the Joplin tornado’s rightward flank.

At this point, the user groups the observed treefall field into regularly-spaced bins, offset and running parallel to the line of maximum damage. The average normalized treefall direction for each bin reveals an average cross-section of normalized tornado-induced treefall. Likewise, this binning procedure is carried out on the modeled treefall vectors and repeated several times for a range of various vortex parameter values until a modeled pattern subjectively matches that of the observed pattern. The vortex model also uses an estimate of the radius of maximum winds from the tornado. The user may estimate this radius via aerial imagery or a ground survey by identifying the region of the damage path where maximum winds and translation speed set as fixed values, the remaining free parameters become the radial and tangential velocities. Karstens et al. (2013) found that a two-to-one ratio of the radial to tangential velocities provided the best matching pattern in the two cases analyzed (one of which was the Joplin tornado), implying that these tornadoes had strong radial near-surface inflow.

Fig. 8 shows an example of this subjective comparison and selection using a bin spacing of 100 m. After making

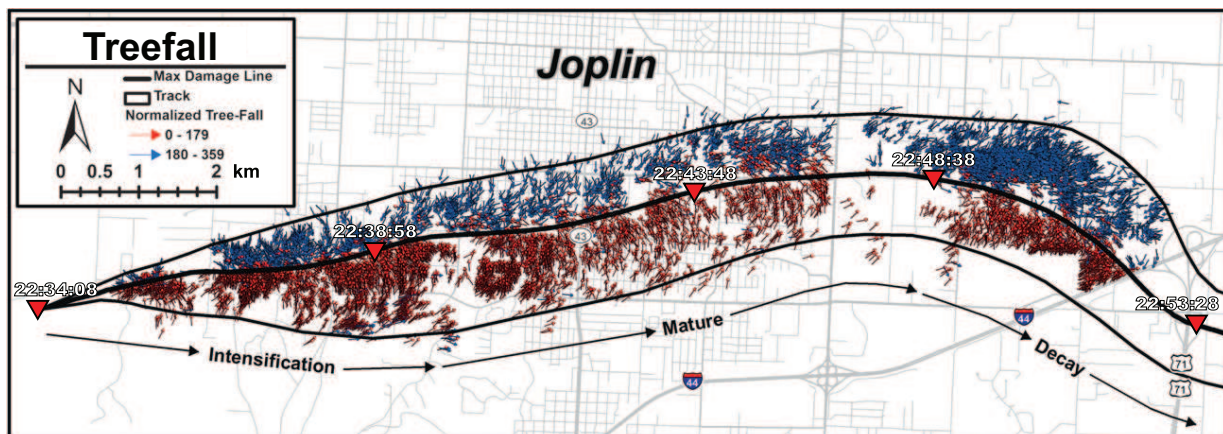


FIG. 7. Digitized geospatial elements necessary for usage of the Karstens method based on the treefall from the 22 May 2011 Joplin, MO tornado. Red triangles and associated UTC times indicate the along-track position of each tornado vortex signature centroid (estimated from the Springfield, MO, [KSGF] Weather Surveillance Radar [WSR]-88D). Adapted from Karstens et al. (2013).

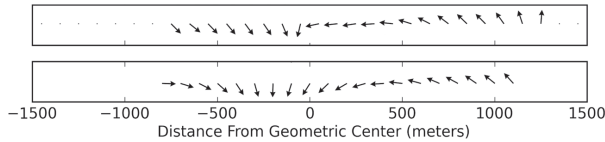


FIG. 8. An example of an observed (top) and modeled (bottom) mean cross-section of normalized tornado-induced treefall vectors. Adapted from Karstens et al. (2013).

a manual selection based on a subjective visual comparison, the wind field produced from the analytical vortex model that produced the modeled treefall pattern leads to an estimate of the maximum wind speed of the tornado across the damage path.

### 3. COMPARISON BETWEEN METHODS

The authors chose the 22 May 2011 Joplin, MO EF5 tornado as the case study with which to conduct the comparison of all three methods simply because the Lombardo and Karstens methods had already been applied to this tornado. All three methods yield estimates of wind speeds as a function of the percentage of trees blown down (Fig. 9). Each of these functions is derived differently. While the lognormal treefall function associated with the Lombardo method is derived directly from data collected within the Joplin tornado track (assumed a constant  $40 \text{ m s}^{-1}$ ), the function associated with the Karstens method is derived solely from a Gumbel distribution (Gumbel 1958) of treefall-inducing wind speeds based on the EF scale (WSEC 2006). The function associated with the Godfrey–Peterson method is derived from ground survey data collected in the Great Smoky Mountains National Park following a 27 April 2011 EF4 tornado and is very similar to the relationship based on ground surveys in the Chattahoochee National Forest. The function shown for the Godfrey–Peterson method in Fig. 9 therefore represents the relationship between the percentage of trees blown down and wind speed for a central hardwoods forest typical of the southeastern United States rather than the somewhat similar oak-hickory forest surrounding Joplin. Nevertheless, the authors feel confident in attempting a broad generalization and applying this relationship to the trees in Joplin. Despite these differences in origin, all three functions exhibit strong similarities in their wind speed estimates, differing by no more than one EF-scale level in all but the smallest percentage of trees blown down. It is important to note that the functions associated with the Lombardo and Karstens methods do not fall consistently within the 95% confidence interval given by the Godfrey and Peterson (2017) approach, but this may be due to the more hardy trees found in Joplin compared with the sheltered trees in southeastern forests. Given the functions shown in Fig. 9, the authors remain confident that any of these three approaches would produce reasonable wind speed estimates based on the percentage of trees blown down.

Application of the Godfrey–Peterson method to the trees in Joplin yields a large swath of EF5 damage (Fig. 10), with the expected reduction in damage levels on the left and right sides of the damage track. Since the approach relies on a sufficient number of trees within each subplot, the most realistic result is obtained with  $200 \text{ m} \times 200 \text{ m}$  subplots. This is larger than the recommended subplot area in dense forests, and sacrifices spatial resolution, but the relative scarcity of trees in this suburban environment necessitates this adjustment. Though the National Weather Service (NWS) rated this tornado EF5 through ground-based damage assessments, the prevalence of EF5 ratings via the Godfrey–Peterson method is likely overinflated due to the shortage of trees in this suburban environment (i.e., the number of trees in each subplot barely exceeds the minimum requirement of 10 trees). This shortage of trees makes it more likely that a subplot will have experienced damage to a larger percentage of the total number of its trees compared with a subplot with an ideal number of trees (i.e., 100 trees) and highlights the limitations of the Godfrey–Peterson method outside a continuously-forested damage track. Also note that there are sections of the tornado track that are not rated by this method because, at fewer than 10 trees per subplot even with the larger subplot area, there are not enough trees to assign an EF-scale rating. As described in Godfrey and Peterson (2017), a spatial shift in the location of each subplot does not appear to make a substantial impact on either the overall distribution of EF-scale levels along the tornado track or the general character of the visual presentation of the damage map.

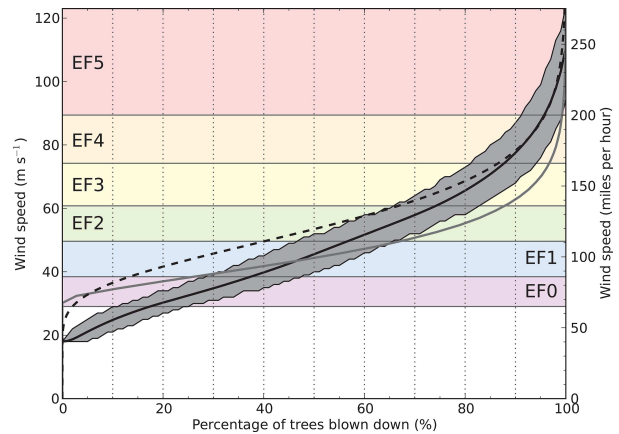


FIG. 9. Wind speed estimates via the Godfrey–Peterson method (solid line, Godfrey and Peterson 2017), the Lombardo method (dashed, Lombardo et al. 2015), and the Karstens method (gray, Karstens et al. 2013) as a function of the percentage of trees blown down. The Godfrey and Peterson (2017) wind speed estimates are based on the tree population in the Great Smoky Mountains National Park, while the Karstens et al. (2013) and Lombardo et al. (2015) wind speed estimates are based on treefall in the 22 May 2011 Joplin, MO tornado. The gray-shaded region denotes the 95% confidence interval based on the Godfrey–Peterson method for each percentage of trees blown down. The colored regions represent the wind speeds associated with each EF-scale level.

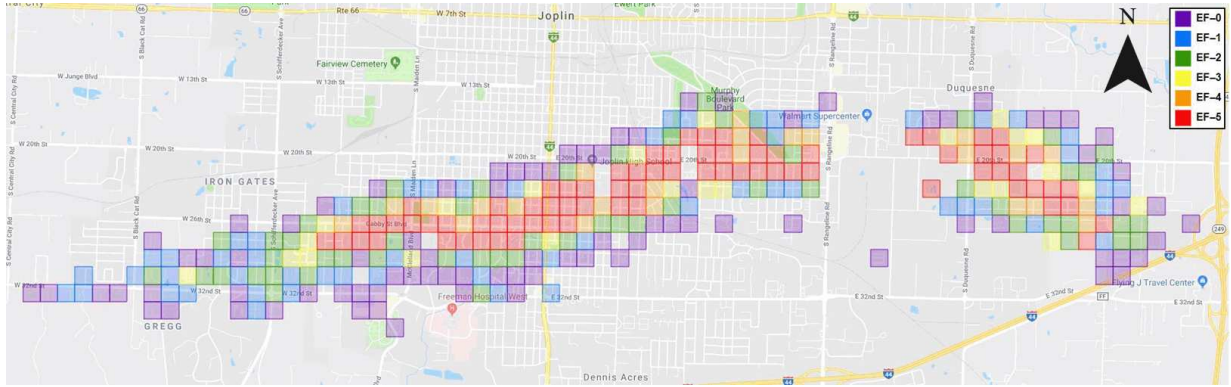


FIG. 10. EF-scale ratings assigned to small 200 m × 200 m subplots along the length of the Joplin tornado track via the Godfrey–Peterson method. The tornado traveled approximately from the west to the east (i.e., left to right).

The Lombardo method produces a map of EF-scale ratings shown via smoothed polygons, much like the polygons drawn in the NWS Damage Assessment Toolkit (Fig. 11). The highest rating for the Joplin tornado via this approach is EF4, which roughly coincides with the swath of highest wind speeds estimated by the Godfrey–Peterson method. In contrast with the Godfrey–Peterson method, the Lombardo method provides continuous ratings through the most damaging portion of the tornado track, regardless of land use.

The Karstens method is applied here to a section of the damage path that coincides with the mature stage of the Joplin tornado (Karstens et al. 2013; Fig. 7) and EF-contours are based on the resulting best match between the modeled and observed averaged cross-sections of treefall (Fig. 12). The highest rating for the Joplin tornado via this approach is EF5 and coincides with the swath of highest wind speeds estimated via the Godfrey–Peterson and Lombardo methods.

Fig. 13 shows an overlay of the wind speed estimates for the Joplin tornado determined via all three methods and is a composite of Figs. 10–12. Despite the very different methodological approaches, each method captures

the spatial characteristics of the wind field, with the maximum wind speeds following near the centerline of the tornado track and roughly coincident EF-scale estimates for the areas on either side of the track.

An appropriate comparison of wind speed estimates should ideally include an estimate of the wind speeds experienced on the ground obtained via some other method. Fortunately, Marshall et al. (2012) conducted a detailed ground assessment along the entire Joplin tornado track (Fig. 14), enabling a comparison of ground-truth EF-scale levels with the EF-scale levels from the three treefall-based wind speed estimation methods presented here. Noting that Marshall et al. (2012) did not include the EF0 contour (hence its conspicuous absence in Fig. 14), it is clear that all three methods do an excellent job of capturing the spatial character of the damage. The Godfrey–Peterson method captures the spatial variability exhibited by the observed damage, though it dramatically overestimates the area of EF5 damage for reasons discussed above and in Godfrey and Peterson (2017). In contrast, the Lombardo and Karstens methods each produce overly-smoothed contours compared with the observations, but this is expected based on the nature

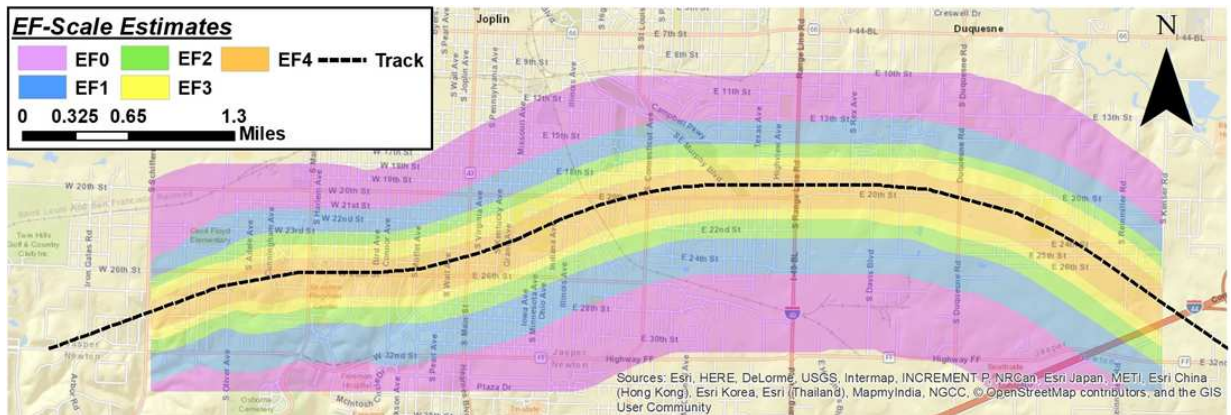


FIG. 11. EF-scale ratings along a portion of the Joplin tornado track via the Lombardo method.

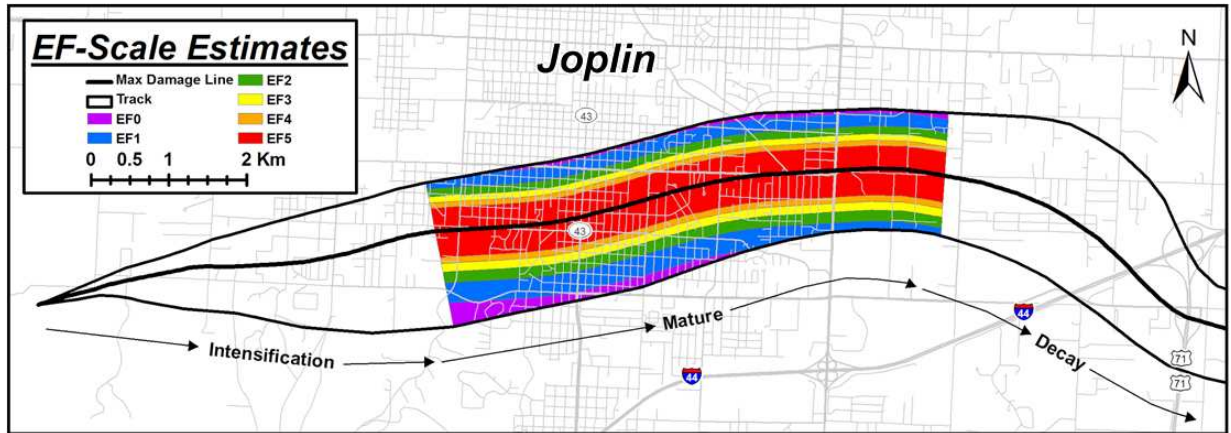


FIG. 12. EF-scale ratings along a portion of the Joplin tornado track via the Karstens method.

of each procedure. The Karstens method also overestimates the wind speeds in the most damaging swath, but this is reasonable given that it is intended to provide the peak wind speed. Indeed, the Karstens method does an excellent job finding the peak wind speeds on either side of the centerline of the tornado, though the region of EF5 winds is perhaps too wide.

Wind speed estimates along a north-to-south transect perpendicular to the path of the Joplin tornado can provide a more direct comparison of the results from each method. Fig. 15 shows wind speeds along tran-

sects across the tornado track at the longitude of the independently-derived maximum estimated wind speed obtained via both the Godfrey–Peterson and the Lombardo methods (see Fig. 13 for the location of the western transect). Note that the wind speed estimates from the Karstens method are derived from the mean cross-section of treefall during the mature stage of the Joplin tornado and can therefore provide a valid comparison with the other methods at this longitude. Given the granularity of the Godfrey–Peterson method and the desire to provide a representative picture of a transect derived

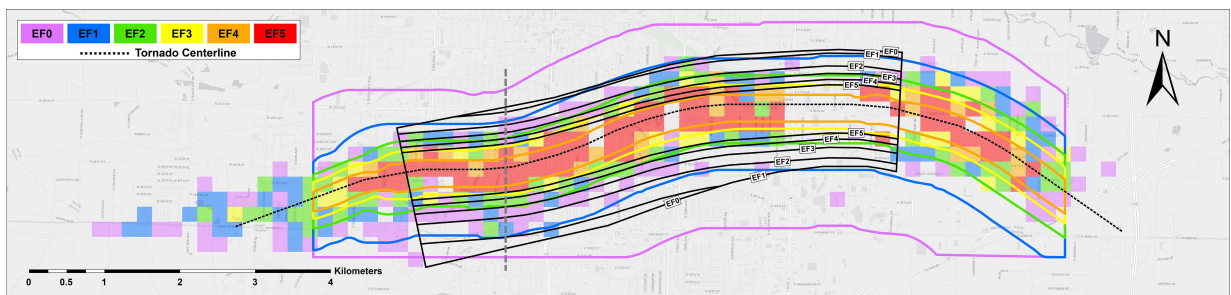


FIG. 13. Comparison of EF-scale ratings along a portion of the Joplin tornado track from the Godfrey–Peterson method (colored grid cells), the Lombardo method (colored lines), and the Karstens method (black lines with labels). The black dashed line is the centerline of the tornado track and the grey dashed line is the location of the western transect shown in Fig. 15.

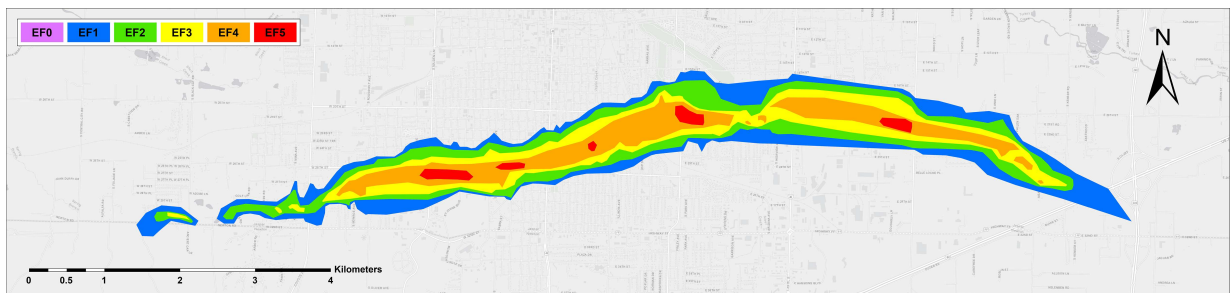


FIG. 14. Damage map developed from a detailed ground assessment of mostly traditional EF-scale damage indicators following the Joplin tornado. Adapted from Marshall et al. (2012).



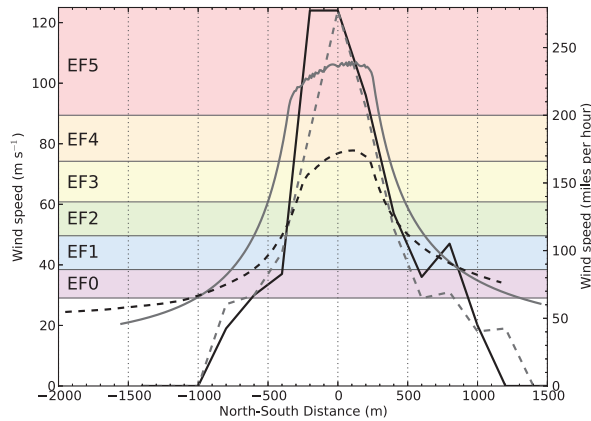


FIG. 15. Wind speed estimates along a north-to-south transect perpendicular to the path of the Joplin tornado obtained via the Godfrey–Peterson method at the longitude indicated in Fig. 13 (solid black) and along the grid cells immediately to the east of the first transect (gray dashed), the Lombardo method (black dashed), and the Karstens method (solid gray). The colored regions represent the wind speeds associated with each EF-scale level.

from this method, Fig. 15 shows two estimates for the Godfrey–Peterson method derived from adjacent transects at both the location shown in Fig. 13 and along the grid cells immediately to the east of the first transect. All three methods produce a transect that indicates that the wind speed is highest on the right side of the tornado, as expected for a tornado with a strong translational motion vector. The Lombardo method underestimates the maximum wind speeds by a full EF-scale level, while the Godfrey–Peterson method appears to underestimate the wind speed at the edges of the tornado at and below the EF0 threshold, compared with each of the other two methods. While the overlapping wind speed estimates at specific points can differ by several EF-scale levels among all three methods, a slight north-to-south shift on the order of a few hundred meters in the assignment of the centerline of the tornado track—or the location of the subplots for the Godfrey–Peterson method—could improve the alignment of these estimates. Nevertheless, the overall character of the wind field appears similar among all three methods.

While each approach for estimating wind speeds via treefall patterns differs in procedural aspects, data collection, and processing requirements, each method produces comparable results with some notable differences as discussed above. This general agreement across the methods supports the application of any one method with confidence. Notably, the similarities exhibited by all three methods support the applicability of a single wind speed–treefall percentage relationship to multiple forest types when applying the Godfrey–Peterson method. Implementation of any treefall-based wind speed estimation method therefore will depend on the data availability, computational resources, and time to invest in obtaining wind speed estimates.

**Acknowledgments.** The authors wish to thank the ASCE Wind Speed Estimation Standards Committee for valuable feedback on portions of this work, as well as G. Alex Flynt for tagging thousands of standing trees in the Joplin tornado track.

## REFERENCES

- Beck, V., and N. Dotzek, 2010: Reconstruction of near-surface tornado wind fields from forest damage. *J. Appl. Meteor. Climatol.*, **49**, 1517–1537.
- Cannon, J. B., M. E. Barrett, and C. J. Peterson, 2015: The effect of species, size, failure mode, and fire-scarring on tree stability. *For. Ecol. Manag.*, **356**, 196–203, doi:10.1016/j.foreco.2015.07.014.
- Godfrey, C. M., and C. J. Peterson, 2017: Estimating enhanced Fujita scale levels based on forest damage severity. *Wea. Forecasting*, **32**, 243–252, doi:10.1175/WAF-D-16-0104.1.
- Gumbel, E. J., 1958: *Statistics of Extremes*. Columbia University Press, 375 pp.
- Holland, A. P., A. J. Riordan, E. C. Franklin, 2006: A simple model for simulating tornado damage in forests. *J. Appl. Meteor. Climatol.*, **45**, 1597–1611, doi:10.1175/JAM2413.1.
- Kane, B., and E. T. Smiley, 2006: Drag coefficients and crown area estimation of red maple. *Can. J. For. Res.*, **36**, 1951–1958.
- Karstens, C. D., W. A. Gallus, B. D. Lee, and C. A. Finley, 2013: Analysis of tornado-induced tree fall using aerial photography from the Joplin, Missouri, and Tuscaloosa–Birmingham, Alabama, Tornadoes of 2011. *J. Appl. Meteor. Climatol.*, **52**, 1049–1068, doi:10.1175/JAMC-D-12-0206.1.
- Kretschmann, D. E., 2010: Mechanical properties of wood. *Wood Handbook: Wood as an Engineering Material*, R. J. Ross, Ed., Forest Products Laboratory General Tech. Rep. FPL-GTR190, Forest Service, 5-15-46. [Available online at [http://www.fpl.fs.fed.us/documnts/fplgtr/fplgtr190/chapter\\_05.pdf](http://www.fpl.fs.fed.us/documnts/fplgtr/fplgtr190/chapter_05.pdf).]
- Kuligowski, E. D., F. T. Lombardo, L. T. Phan, M. L. Levitan, and D. P. Jorgensen, 2014: Technical Investigation of the May 22, 2011, Tornado in Joplin, Missouri. Final Report NIST NCSTAR 3, National Institute of Standards and Technology (NIST), 428 pp.
- LaDue J. G., J. Wurman, M. Levitan, F. T. Lombardo, C. D. Karstens, J. Robinson, and W. Coulbourne, 2018: Advances in Development of the ASCE/SEI/AMS Standard for Wind Speed Estimation in Tornadoes and Other Windstorms. 29th Conference on Severe Local Storms. Stowe, VT, 29 [Available online at <https://ams.confex.com/ams/29SLS/webprogram/Paper348726.html>.]
- Letzmann, J. P., 1923: Das Bewegungsfeld im Fuß einer fortschreitenden Wind-oder Wasserhose (The flow field at the base of an advancing tornado). Ph.D. thesis, University Helsingfors, Acta et Commentationes Universitatis Dorpatensis AVI.3, 136 pp. [Available online at <http://essl.org/pdf/Letzmann1923/Letzmann1923.pdf>.]
- Letzmann, J. P., 1925: Fortschreitende Luftwirbel (Advancing air vortices). *Meteorol. Z.*, **42**, 41–52.
- Letzmann, J. P., 1939: Richtlinien zur Erforschung von Tromben, Tornados, Wasserhosen und Kleintromben (Guidelines for research on tornadoes, waterspouts, and whirlwinds). *Klimatologische Kommission, IMO Publ. 38*, Secretariat de l'Organisation Météorologique Internationale, Ed., Edouard Ijdo, 91–110. [Available online at <http://essl.org/pdf/Letzmann1939/Letzmann1939.pdf>.]

- Lewellen, D. C., 2012: Effects of topography on tornado dynamics: A simulation study. Preprints, 26th Conference on Severe Local Storms, Nashville, TN, Amer. Meteor. Soc., 4B.1. [Available from <https://ams.confex.com/ams/26SLS/webprogram/Paper211460.html>.]
- Lombardo, F. T., D. B. Roueche, and D. O. Prevatt, 2015: Comparison of two methods of near-surface wind speed estimation in the 22 May, 2011 Joplin, Missouri Tornado. *J. Wind Eng. Ind. Aerodyn.*, **138**, 87–97.
- Marshall, T. P., W. Davis, and S. Runnels, 2012: Damage Survey of the Joplin Tornado: 22 May 2011. 26th Conference on Severe Local Storms. Nashville, TN, 6.1 [Available online at <https://ams.confex.com/ams/26SLS/webprogram/Paper211662.html>.]
- Nicoll, B. C., B. A. Gardiner, B. Rayner, and A. J. Peace, 2006: Anchorage of coniferous trees in relation to species, soil type, and rooting depth. *Can. J. For. Res.*, **36**, 1871–1883, doi:10.1139/x06-072.
- Panshin, A. J., and C. de Zeeuw, 1970: *Textbook of Wood Technology*. 3rd ed. McGraw-Hill, 705 pp.
- Peltola, H., 2006: Mechanical stability of trees under static loads. *Amer. J. Botany*, **93**, 1501–1511.
- Peltola, H., and S. Kellomaki, 1993: A mechanistic model for calculating windthrow and stem breakage of Scots pine at stand edge. *Silva Fenn.*, **27**, 99–111.
- Peltola, H., S. Kellomaki, and V.-P. Ikonen, 1999: A mechanistic model for assessing the risk of wind and snow damage to single trees and stands of Scots pine, Norway spruce, and birch. *Can. J. For. Res.*, **29**, 647–661.
- Peterson, C. J., and V. Claassen, 2013: An evaluation of the stability of *Quercus lobata* and *Populus fremontii* on river levees assessed using static winching tests. *Forestry*, **86**, 201–209, doi:10.1093/forestry/cps080.
- Purves, D. W., J. W. Lichstein, and S. W. Pacala, 2007: Crown plasticity and competition for canopy space: A new spatially implicit model parameterized for 250 North American tree species. *PLoS One*, **2**, e870, doi:10.1371/journal.pone.0000870.
- Rhee, D. M., and F. T. Lombardo, 2018: Improved near-surface wind speed characterization using damage patterns. *J. Wind Eng. Ind. Aerodyn.*, **180**, 288–297.
- WSEC, 2006: A recommendation for an enhanced Fujita scale (EF-scale). Texas Tech University Wind Science and Engineering Center Rep., 95 pp. [Available online at [www.depts.ttu.edu/weweb/pubs/efscale/efscale.pdf](http://www.depts.ttu.edu/weweb/pubs/efscale/efscale.pdf).]